https://doi.org/https://doi.org/10.1016/j.ijimpeng.2015.09.005

The unexpectedly small coefficient of restitution of a two-degree-of-freedom mass-spring system and its implications

H.H. Ruan[a*] and T.X. Yu[b]

[a] Department of Mechanical Engineering, The Hong Kong Polytechnic University, Hung Hom, Kowloon, Hong Kong

[b] Department of Mechanical and Aerospace Engineering, The Hong Kong University of Science and Technology, Clear Water Bay, Kowloon, Hong Kong

Abstract

When two elastic solids collide each other, the coefficient of restitution (COR) is generally considered to be unity based on the notion that the elastic strain energy will be fully released and the kinetic energy and momentum are conserved. This statement, with the support of numerous experiments of ball collision, is so widely acknowledged that people rarely realize that the COR of pure elastic collision can be significantly smaller than unity under some circumstances. The missing part in the story is the vibrational energy stored in the reciprocal motion of materials or structural components relative to the centre of mass. This article is to unveil the striking effect of elastic vibration using the most concise mass-spring system and demonstrate that the COR can even be as small as 0.178. We then discuss the effects of plasticity, non-linear elasticity and increased number of degrees of freedom and conclude the implication of small COR in crashworthiness design.

Keywords

Coefficient of Restitution (COR), Mass-Spring system, Crashworthiness, Energy absorption

* Corresponding author: hhruan@polyu.edu.hk

1. Introduction

When two solids collide with a relative velocity V_r and separate with a updated relative velocity V_r' (in the direction opposite to V_r), the kinematic coefficient of restitution (COR) upon Newton's definition is the ratio of these two velocities $e_k = V_r'/V_r$. COR had long been regarded as an empirical or material parameter for solving the collision of two solids. Its applicability is based on the assumptions that the velocity change is instantaneous and that the relative velocity does not change the line of direction. Therefore the kinematic COR is insufficient in solving collision problems involving friction and slip and may even lead to unphysical result [1]. Stronge [2] then redefined COR from the energetic sense, namely the square root of the ratio between the energy release during restitution and the energy absorbed by deformation during compression. The two definitions of COR are equivalent for frictionless collision of rigid or very stiff bodies. When the stiffness is small and vibration is significant, the statement that strain energy releases to kinetic energy becomes ill-posed since vibrational degree of freedom (DOF) may preserve a portion of energy and probably bring about multiple collisions, but the kinematic COR still holds if the velocity of centre of mass is used. In so doing, the kinematic COR is also the ratio of the magnitudes of momentum after and before collision, which is unambiguously defined even with vibration and will be used in following analysis and discussions.

In the scenario involving vibration, one can immediately think of that the COR must be less than unity even though the bodies in collision are purely elastic [3, 4]. If vibration is induced before collision, e.g., the thermal vibration of a nanocluster, the COR can even be larger than unity [5, 6] since a portion of energy can be transferred from vibrational DOF to translational DOF. Lately, Müller *et al*. [7] illustrated the striking and unexpected effect of vibration on COR based on an experimental study of collision between steel ball and glass panel. After a statistical study of thousands of collisions, they found a stepwise change of COR with impact velocity and unveiled that the width and height of steps are consistent with the vibrational frequency and amplitude of the glass panel respectively. Although these investigations exhibit the remarkable effect of vibration on COR, the argument that "elastic collision" leads to unity COR is still deeply grafted in people's mind by textbook picture of collision of two spheres. The collision of spheres certainly cannot be the representative of structural collisions. For example, an experimental study of collision between an aluminium ring and a rigid anvil showed that the COR is about 0.5 when the impact velocity is less than the yield velocity of the material [8]. Bao and Yu [9] further indicated, through numerical simulation, that the COR of an elastic ring is around 0.78 if the impact speed is very low. However, the unanswered question is how significant the effect of vibration on COR in structural collisions can be, which thus motivates this work. Before specifying the theoretical model of investigation, we shall briefly review the studies

concerning COR in different systems.

Many modern studies of the effect of COR contributed to the understanding of granular matter. For them the COR is one of the most fundamental parameters, which was specified based on studies of collision of two spheres. Hertz's contact theory was reformulated to consider the inertial effect [10, 11]. The COR resulted, considering vibration [10] and elastic waves in solids [12, 13], was very close to one. Unity COR was used in the classical kinetic theory of isothermal gases, as first formulated by Boltzmann. In order to establish the relation between the conserved kinetic energy and temperature, Boltzmann assumed *molecular chaos,* namely that the collisions are spatially and temporally uncorrelated. In recent developments of many-particle kinetics, viscous force is involved to describe cooling or slowdown of granular gases [14-17]. The introduction of viscous force leads to many interesting phenomenon of particle dynamics. For example, particles may aggregate to form structures and the distribution of particle velocities is no longer Maxwellian [18].

COR plays important role not only for granular gases but also for granular materials. The latter exhibit a rich variety of behaviour ranging from solid-like to liquid-like, depending on the external stresses applied to them. Under stresses, a granular system deforms and dissipates energy, which microscopically is due to the viscous forces in grain collisions. In order to quantify the effect, many efforts were devoted to solving the collision between viscoelastic spheres [10, 14-16]. However the solution was nontrivial owing to the intermingling of inertia effect and viscous force. Generally assumed were that the dynamic deformation profile is identical to the static one and that the relaxation time is much shorter than the collision duration [10, 14, 16]. Based on these assumptions, the normal collision between viscoelastic spheres was solved [14] and the resulted COR, though still complicated, can at least be numerically calculated [15, 16]. Recently Brilliantov *et al*. [17] release the quasi-static assumption and resolve the problem using perturbation theory. The cause of viscous force is the internal vibration modes excited by collision. This was derived by Morgado and Oppenheim [19] using the first-principle theory and studied more extensively by Murakami and Hayakawa [3] using a hybrid approach combining continuum mechanics and molecular dynamics.

Many molecules are far from sphere but possess spatial structures. This fact stimulated the investigation of COR of a chain of particles linked by linear springs [20], where Basile *et al*. found that a large portion of the initial kinetic energy was "lost" into the vibration of the chain when the chain is short with only several particles. This "loss" approaches zero when the length of chain increases. Nagahiro and Hayakawa [21] further indicated that COR would be velocity dependent if the springs are nonlinear.

In granular dynamics, plasticity is rarely involved since the irreversible deformation changes the

geometry of sphere, which brings about the geometrical effect and makes the multi-particle problem more daunting. But for macroscopic collisions, plastic deformation is the main concern. The early studies (before 1960s) on COR were to characterize dynamic strengths of materials. Some of those studies were summarized in the monograph by Johnson [11]. With the development of more accurate approach (e.g., the Split-Hopkinson Pressure Bar) for characterizing dynamical strengths of materials, the plasticity-induced velocity dependence of COR is less used or studied. Some recent studies concerned COR of sports balls, e.g., table tennis balls [22, 23] or tennis balls [24, 25]. But in most investigations concerning behaviours of structures subjected to large dynamic loads due to impact or collision, COR is the least considered parameter [26] because of the notions that elastic deformation cannot dissipate energy and that structural vibration cannot absorb a large portion of kinetic energy either. The consensus is that when a structure, say a car, crashes onto a rigid wall, a portion of kinetic energy is dissipated through plastic deformation of structures and the rest is kept after rebound. Therefore, rigid plastic assumption was commonly used [27] and structural vibration was neglected. Is vibration really useless in crashworthiness? To clarify this doubt, we shall also query the maximum effect of vibration on COR.

The extensive investigations of granular collisions (see for example [3]) have exhibited that collision can lead to a significant energy transfer from the translation motion to vibrational modes in some circumstance, leading to a small COR. This result inspires us to consider another scale of collision: the collision of engineering structures. Different from small atomic systems (say the nanoparticles [3]), an engineering structure is composed of masses and supporting frames. Different configuration of them affects the impact induced dynamic behaviours. We are interested in the question whether the collision onto a wall can also result in a significant energy transfer from the translation motion to structural vibrations and a small COR. To answer this question, let us first simplify engineering structures to several lumped masses and connection springs.

2. Two-DOF Model

2.1 Analytical solution

The simplest model for evaluating the effect of vibrational DOF on COR is the two-DOF system shown in Fig. 1. The system contains two masses m_1 and m_2, and a structural spring of the potential U_2. At the moment of collision, $t = 0$, the mass m_1 contacts with the rigid wall and the displacements u_1, u_2 and u_0 refer to the position change of mass m_1, m_2 and the wall respectively. The positive direction, as shown, is defined to be leaving the wall. If the collision or the change of velocity occurs in no time, the COR after the first collision between the mass m_1 and the wall is:

$$e_1 = \frac{m_1 V_0 - m_2 V_0}{(m_1 + m_2) V_0} = \frac{1-\alpha}{1+\alpha}, \tag{1}$$

where $\alpha = m_2/m_1$ and the superscript "1" means the kinematic COR after first collision. The mass ratio α represents the mass distribution at the contact front and the rear structures, which may be varied in a wide range in engineering structures. For example, the α of a rear-engine car may be much larger than that of a front-engine car. According to Eq. (1), e_1 reduces with α and approaches zero when α approaches unity. This quick analysis has indicated that COR may be very small if vibrational DOF is involved. However, the harmonic motion of m_1 can result in multiple collisions with the wall and exchanges of energy between vibrational and translational DOFs. The solution of multiple collisions is nontrivial and leads to very rich dynamic behaviour of the two-DOF system. Therefore, we detail the analytical solution as follows. In order to make the effect of vibration more transparent, we use the following canonical coordinates to differentiate the translational and vibrational DOFs:

$$\begin{aligned} p_1 &= (m_1\dot{u}_1 + m_2\dot{u}_2) \\ p_2 &= (m_1\dot{u}_1 - m_2\dot{u}_2) \\ q_1 &= (u_1 + u_2)/2 \\ q_2 &= (u_1 - u_2)/2 \end{aligned}. \tag{2}$$

The the Hamiltonian of the two-DOF system is:

$$H = \frac{1}{8m_1}(p_1 + p_2)^2 + \frac{1}{8m_2}(p_1 - p_2)^2 + U_2(-2q_2) + U_1(q_1 + q_2 - u_0),$$

where the potential U_1 governs the contact between m_1 and the wall. If the system is assumed purely elastic, both potentials are merely function of instantaneous deformation, namely, $U_1 = U_1(u_1 - u_0)$ and $U_2 = U_2(u_2 - u_1)$. The governing equations are:

$$\begin{aligned} \frac{\partial H}{\partial p_1} &= \frac{1}{4m_1}(p_1 + p_2) + \frac{1}{4m_2}(p_1 - p_2) = \dot{q}_1 \\ \frac{\partial H}{\partial p_2} &= \frac{1}{4m_1}(p_1 + p_2) - \frac{1}{4m_2}(p_1 - p_2) = \dot{q}_2 \end{aligned}, \tag{3a, b}$$

$$\begin{aligned} \frac{\partial H}{\partial q_1} &= \frac{\partial U_0}{\partial q_1} = F_1(q_1 + q_2 - u_0) = -\dot{p}_1 \\ \frac{\partial H}{\partial q_2} &= \frac{\partial U_1}{\partial q_2} + \frac{\partial U_0}{\partial q_2} = -2F_2(-2q_2) + F_1(q_1 + q_2 - u_0) = -\dot{p}_2 \end{aligned}, \tag{4a, b}$$

where the overhead dot (say $\dot{q}$) indicates time derivative, $F_i(x) = U_i'(x)$ are spring forces, and the prime indicates differentiation with respect to the mere variable. Eq. 4(a) describes the detailed momentum change of the system during a finite collision time. But if the contact spring is elastic and sufficiently rigid, *i.e.*, $\beta = F_2'(x)/F_1'(x) \to 0$, the detail of contact is negligible and the velocity change of m_2 is only governed by the conservation of momentum and kinetic energy. During separation the contact spring does not work, Eq. 4(b) reduces to

$$\dot{p}_2 + 4k_2q_2 = \dot{p}_2 + \omega Q_2 = 0, \tag{5}$$

where we have assumed the linear response of structural spring $F_2(x)=k_2x$ and defined $\omega=\sqrt{k_2/m_1+k_2/m_2}$ the nature frequency of the 2-DOF system. In Eq. (5), the term $Q_2=4k_2q_2/\omega$ is defined to absorb the constant $4k_2/\omega$, so that the subsequent expressions will not depend on a particular k_2. Differentiating Eq. (5) and substituting 3(a) and 3(b) render:

$$\ddot{p}_2+\omega^2 p_2-\omega^2 e_1 p_1=0, \tag{6}$$

where we have substituted $e_1=\dfrac{1-\alpha}{1+\alpha}$ for shorthand.

We then use the inertia frame of the velocity -V_0 so that the wall moves toward the stationary mass-spring system at the speed of V_0. The first collision occurs at t_1=0, before which $p_1(t_1^-)=p_2(t_1^-)=0$. If the contact spring is infinitely stiff, the collision renders the immediate change of momentum: $p_1(t_1^+)=p_2(t_1^+)=2m_1V_0$ and initial compression of the spring $q_2(t_1^+)=0$. For clarity and brevity, we use the superscripts "*n*-" and "*n*+" to denote the magnitude of a variable before and after the *n*th collision, respectively. Without a superscript (*n*- or *n*+), the variable should be regarded to be time dependent. The solution of Eqs. (5) and (6) after the first collision is:

$$p_1=p_1^{1+},\quad p_2=e_{k1}p_1^{1+}(1-\cos\omega\Delta t_1)+p_1^{1+}\cos\omega\Delta t_1,\text{ and }\quad Q_2=(1-e_{k1})p_1^{1+}\sin\omega\Delta t_1 \tag{7a, b, c}$$

where $\Delta t_1=t-t_1^+$ is the time elapse after the first collision. Substituting above equation into Eq. (3) renders

$$\dot{u}_1=\dot{q}_1+\dot{q}_2=\frac{p_1+p_2}{2m_1}=\frac{2V_0}{1+\alpha}(1+\alpha\cos\omega\Delta t_1) \tag{8}$$

The distance between the mass 1 and wall (or the elongation of the contact spring) is:

$$s_1=u_1-V_0\Delta t_1=\frac{\alpha V_0\Delta t_1}{(1+\alpha)}\left(2\frac{\sin\omega\Delta t_1}{\omega\Delta t_1}-1+\frac{1}{\alpha}\right). \tag{9}$$

We then identify the minimum of *s* by taking $ds_1/d(\Delta t_1)=0$, which renders:

$$2\cos\omega\Delta t_1^*=1-1/\alpha, \tag{10}$$

where Δt_1^* is the moment that s_1 minimizes. The occurrence of second impact requires $s_1^{\min}<0$ when

$\Delta t_1^* > 0$. Note that if the second collision does not occur during the first period of the structure vibration, there will not be any more collisions and the COR after the first collision is e_{k1}. The marginal case is $s_1^{\min} = 0$. Since Eq. (10) is the condition for the minimum of *s*, substituting it into Eq. (9) to remove α and letting $s_1 = 0$ result in:

$$\tan\left(\omega\Delta t_1^*\right) = \omega\Delta t_1^*, \tag{11}$$

This equation has infinite positive roots of $\omega\Delta t_1^*$. They are 4.49341, 7.72525, 10.9041… , while the first one, $\omega\Delta t_1^* = 4.49341$, is the only valid solution since it is within the first period of the structure vibration and renders the global minimum of *s.* Using Eq. (10), we obtain the value of α for the first minimum of COR, $\alpha_1^* = 0.6971$, and the minimum COR as 0.178481. With the increase of α, there will be more collisions. We then consider the consequence of the *n*th collisions. At the moment right before the *n*th collision, the relative velocity between the mass 1 and the wall is:

$$\dot{u}_1^{n-} - V_0 = \frac{p_1^{n-} + p_2^{n-}}{2m_1} - V_0 = \frac{p_1^{n-} + p_2^{n-} - p_1^{1+}}{2m_1}, \tag{12}$$

After the collision, the change of momentum $-2m_1\left(\dot{u}_1^{n-} - V_0\right)$ all goes to the mass 1. Therefore:

$$p_1^{n+} = p_1^{1+} - p_2^{n-},\ p_2^{n+} = p_2^{(n-1)-},\ \text{and}\ \ Q_2^{n+} = Q_2^{n-} \tag{13a, b, c}$$

The solution of equations (5) and (6) after the *n*th collision is:

$$p_1 = p_1^{n+},\quad p_2 = e_{k1}p_1^{n+}\left(1 - \cos\omega\Delta t_n\right) + p_2^{n+}\cos\omega\Delta t_n - Q_2^{n+}\sin\omega\Delta t_n, \tag{14a, b}$$

and

$$Q_2 = -\left(e_{k1}p_1^{n+} - p_2^{n+}\right)\sin\omega\Delta t_n + Q_2^{n+}\cos\omega\Delta t_n \tag{14c}$$

where $\Delta t_n = t - t_n^+$. Using Eqs. 14(a) and (b), the relative distance between the rigid wall and mass 1 is

$$s_n = \int_0^{\Delta t_n}\dot{u}_1 dt - V_0\Delta t_n = \frac{1}{2m_1}\left(\int_0^{\Delta t_n}\left(p_1 + p_2\right)dt - p_1^{1+}\Delta t_n\right) = \frac{1}{2m_1}\int_0^{\Delta t_n}\left(p_2 - p_2^{n-}\right)dt \tag{15}$$

If the further collision does not occur, namely $s_n^{\min} > 0$, the COR after *n*th collisions is

$$e_n = \frac{p_1^{n+}}{(1+\alpha)m_1 V_0} - 1 = e_1 - \frac{2p_2^{n-}}{(1+\alpha)p_1^{1+}}, \tag{16}$$

where Eq. (13a) has been used. In order to find the minimum COR after the *n*th collision, we shall employ the conditions $s_n^{\min} = 0$ when $p_2 = p_2^{n-}$. In detail, let Δt_n^* be the moment that *s* minimizes, the conditions for a COR minimum are

$$p_2 = e_1 p_1^{n+}\left(1 - \cos\omega\Delta t_n^*\right) + p_2^{n+}\cos\omega\Delta t_n^* - Q_2^{n+}\sin\omega\Delta t_n = p_2^{n-}, \tag{17}$$

and

$$2m_1\omega s_{\min} = \left(e_1 p_1^{n+} - p_2^{n-}\right)\omega\Delta t_n^* - \left(e_1 p_1^{n+} - p_2^{n+}\right)\sin\omega\Delta t_n^* + Q_2^{n+}\left(\cos\omega\Delta t_n^* - 1\right) = 0 \tag{18}$$

The complete solution of Eqs. (17) and (18) needs recursive calculation of p_2^{n-} and Q_2^{n-}, which can only be done when α is specified. Therefore, we scan a wide range of α and obtain the analytical result for the case of $\beta = 0$ as shown in Fig. 2(a). The first three minima of COR are 0.178, 0.557, 0.710, which occur at α = 0.697, 2.07, 3.64 respectively. Every minimum of COR corresponds to a sharp change of the trend of COR, which is due to the increase of the number of collisions. With the same number of collisions, the COR increases first from a minimum to unity and then decreases to the next minimum. The maximum COR are always unity. For *n* collisions, Eq. (16) leads to $p_2^{n-} = -\alpha p_1^{1+}$ for the unity COR. The case of $n = 2$ is straightforward. Using Eq. 5(b), $p_2^{2-} = -\alpha p_1^{1+}$ leads to $1 + \alpha^2 - 2\alpha\cos\omega\Delta t_1^{2-} = 0$. Since $\left|\cos\omega\Delta t\right| \le 1$, the only solution is $\alpha = 1$ and $\omega\Delta t_1^{2-} = \pi$. Therefore, when two masses are identical and move towards to wall (employing a stationary inertia frame), the first collision converts the mechanical energy from translational DOF to vibrational DOF and the second collision converts back. Fig. 2(a) also shows that when the number of collision increases, COR oscillatorily approaches unity. The above analytical solution is for cases of $\beta = 0$. In order to have a sense of how well it approximates the small β scenarios, we conducted numerical simulation for finite β using the Verlet integration of the governing equations (3) and (4). The results are also included in Fig. 2. The comparison confirms the analytical solution and show that the results of $\beta = 0$ are accurate for cases of $\beta < 0.01$. When β further increases, the COR minimum reduces and the position of

peak (the magnitude of α) shifts. If the stiffness of the structure spring is comparable to that of the contact spring, say $\beta = 1$, the COR becomes close to 1 and the minimum COR shifts to larger α (~ 3.5).

Owing to multiple collisions, the total duration of collision t_{col} (the subscript "col" means collision), namely the time between the moment of first contact and the moment of complete separation, is no longer infinitesimal even for the case of $\beta = 0$ but dependent on the α. This dependence is shown in Fig. 2(b), in which t_{col} is normalized by the nature period of the two-DOF system. In general the normalized duration ωt_{col} increases with α, which is owing to the jumps of t_{col} when the number of collision increases. But for the same number of collision, ωt_{col} reduces with α since the increase of m_2 renders more momentum towards the wall and makes collision occur earlier. Also shown in Fig. 2(b) is the variation of ωt_{col} in cases of finite β. The overall trend is same as the case of $\beta = 0$. The difference is that the contact process takes time even for single collision. For a very small α, the normalized duration of collision approaches $\frac{\omega t_{col}}{2\pi} = \frac{1}{2}\sqrt{\beta\frac{1+\alpha}{\alpha}}$, which are the intercepts at vertical axis for different values of β.

2.2 Approximate solution

Though the two-DOF system is fundamentally simple, the COR can hardly be obtained based on intuition. The exact solution needs some effort in numerical computation. Herein we suggest an approximate calculation of COR based on detailed observation of Fig. 2(a).

First, the increase of the number of collision with α is depicted in Fig. 2(b). For the case of n collisions, there is only one value of α, denoted by $\alpha^{\#}$, leading to the unity COR. The relation between n and $\alpha^{\#}$ can be closely fitted by a power law:

$$n = 1 + \left(\alpha^{\#}\right)^{0.8}, \tag{19}$$

as shown in Fig. 2(b). The correspondence between the minimum COR and α is also collected in Fig. 2(b). The minima are well fitted by the equation $e = \left(\alpha^{*} - 0.4\right)/\left(1 + \alpha^{*}\right)$, where the superscript "*" designates the minimum COR scenario. Noting that $2\alpha_1^{*} - 1 \cong 0.4$, we may recast the equation as $e = 1 - 2\alpha_1^{*}/\left(1 + \alpha^{*}\right)$. This gives us the idea to express the variation of COR as

$$e = 1 - 2\gamma/\left(1 + \alpha\right) \tag{20}$$

where γ is a function of α and varies between 0 and α_1^*. For scenarios of n collisions,

$$\frac{\gamma}{\alpha_1^*} = \begin{cases} \left(\left(\alpha_n^\# - \alpha\right)/\left(\alpha_n^\# - \alpha_{n-1}^*\right)\right)^{\eta_1}, & \alpha_{n-1}^* \le \alpha < \alpha_n^\# \\ \left(\left(\alpha - \alpha_n^\#\right)/\left(\alpha_n^* - \alpha_n^\#\right)\right)^{\eta_2}, & \alpha_n^\# \le \alpha < \alpha_n^* \end{cases}, \tag{21}$$

The variation of ($\alpha_n^* - \alpha_n^\#$) against n is shown in Fig. 2(c), in which the curve with the expression

$$\alpha_n^* - \alpha_n^\# = n^{0.21} \tag{22}$$

closely fits the data points. Therefore, α_{n-1}^*, α_n^*, and $\alpha_n^\#$ in Eq. (21) can be determined for cases of n collisions using Eqs. (19) and (22). The powers η_1 and η_2 in Eq. (21) are merely to control the curvature of approximated COR curve. With $\eta_1 = \eta_2 = 2$, Fig. 2(d) compares the approximate and exact solutions (for β = 0), which indicates a very good agreement.

3. Extension of 2-DOF model to more realistic models

The two-DOF mass-spring system is not only a toy model to understand the effect of vibrational DOF on COR but also a useful approximation of dynamic response of structures [28]. In the case that the structural response can approximately be described by a time-independent deformation mode and a time-dependent scaling function, the correspondence between the mass-spring system and the structure, in terms of the identicalness of governing equation, can even be established [29]. This approach has been known as the modal approximation technique, as first proposed by Martin and Symonds [30] and extendedly used since then for studying both rigid perfectly plastic and even elastoplastic responses of structures [28].

In actual collisions, the structural response may be non-linear and inelastic and the contact response may not be instantaneous and non-dissipative. In the following we will discuss the scenarios that the contact is non-rigid and even dissipative, that the structural spring is non-linear, and that the number of vibrational DOF is more than one. Through these case studies we shall address the implication of the small COR system in crashworthiness design.

3.1 Effect of β and dissipative contact spring

The Increase of β makes the wall more resembling a soft cushion and induces less structural vibration. Therefore, a larger β leads to larger COR, which has been exhibited in Fig. 2(a). When β =1, the smallest COR is 0.91 occurring at α=3.42. When β is even larger (say β > 10), COR becomes almost unity for any α. The increase of β not only changes of magnitude of COR but also shifts the position of COR minima. The combination of these two effects leads to non-monotonic change of COR with β for a given α. For example, Fig. 3(a) shows the variations of COR with β for α = 2, 2.2 and 2.5 respectively. Along with the increase of β, the sharp minima of COR also appears. These minima are also due to the step change of the number of collision. For manifestation, Fig. 3(b) shows the dimensionless compression (negative) of the contact spring $\omega s_1/V_0$ versus scaled time ωt for cases of β = 0.09, 0.1 and 0.11 and α = 2.2 respectively. The marginal scenario that the third collision is about to occur happens at β = 0.1, rendering one of the COR minima in Fig. 3(a). It should be noted that the increase of β tends to reduce the number of collisions, as shown in Fig. 3(b). This trend is contrary to the effect of α and is also the result of cushion effect of large β.

The contact spring is to represent the fore-displacement response of both the wall and the frontal structure at contact. In structural collisions, e.g., a vehicle crashes onto a wall, plastic deformation is unavoidable due to large velocity discontinuity and limited material strength. The more energy dissipation due to plastic deformation certainly leads to the less COR. However, the effect of plasticity shall be different from the effect of β, since the latter is only the stiffness ratio. One may intuitively think that the kinetic energy is only dissipated at the first collision since the velocity difference at the first collision is plausibly the largest. This is however only valid for small α since larger α leads to more collisions and more dissipation. But we may still define a nominal dissipation ratio (DR) only considering the velocity change of m_1 after the first collision: $DR = 1 - \left(\dot{u}_1^{1+}\right)^2 / V_0^2$. For small α, the first collision results in $e_{1p} = \left(\sqrt{1-DR} - \alpha\right) / \left(1+\alpha\right)$, where the subscript p indicates the effect of plasticity. If no further dissipation occurs, the maximum COR will be resulted from the scenario that all mechanical energy converts from the vibrational DOF to translational DOF, which gives the upper bound of COR:

$$e_{p\max} = \sqrt{1 - \frac{DR}{1+\alpha}}. \tag{23}$$

In order to get a glimpse of the detailed effect of plasticity, we assume that the contact spring follows a power law at loading: $F_1(x) = \kappa x^{\eta}$ and is linear at unloading with the unlading spring constant $k_1 = k_2/\beta$. The loading-unloading curve is exemplified in Fig. 4(a) for different η and the effect of DR is shown in Fig. 4(b) with $\eta = 0.5$. It is shown that the larger DR leads to the smaller COR in general and that positions of COR minima, in terms of α, shift to the smaller α side with the increase of DR, since the rigid wall can catch up the mass more easily.

If a DR is specified, we conceive that the dependence of COR on α will be similar to the case of no dissipation but upper bounded by Eq. (23). The simulation result for the case of $\beta = 0.01$ is shown in Fig. 4(c), which confirms our notion. We chose different values of κ and η in the simulation and found that κ has no effect on COR variation (not able to shown since all curves coincide). But the effect of the power η is prominent: the larger η makes COR approaching the $e_{kp\max}$ quicker with the increase of α. This is because the larger η leads to the quicker increase of the contact force and less dissipation. The effect of η indicates that the reload of the contact spring in multiple collisions may go beyond the first achieved maximum force and lead to additional dissipation in the later collisions. This is more apparent when β becomes larger. Fig. 4(d) shows the case of $\beta = 0.1$, where the COR decreases with α when α is large and η is small.

3.2 Effect of nun-linearity of the structural spring

The structural spring between the two masses can also be non-linear and inelastic. Herein, we pay our attention to the effect of non-linear elasticity since it is ubiquitous in actual structures. Although plasticity and viscoelasticity are also unavoidable, their roles are very straightforward, which dissipates the mechanical energy associated with the vibrational DOF and reduces COR.

The non-linearity must be specified with a specific mechanical design. Therefore, we consider the scissor-like structural spring as shown in Fig. 5(a) (upper inset). This scissor-like spring has recently been studied, e.g., by Sun et al. [31], which was shown to have very good performance in vibration isolation. For this structural spring, the force F_2 and displacement x_2 are related implicitly through the half angle between two hinged bars, θ, which are given by:

$$F_2(x_2) = 2k_s L\cos\theta\left(\frac{\sin\theta_0}{\sin\theta} - 1\right) \quad \text{and} \quad x_2 = \Delta H = 2L(\cos\theta - \cos\theta_0), \tag{24a, b}$$

where L is the length of the bar, k_s is the spring constant and θ_0 is the initial half angle between two hinged bars when the spring is not loaded. When the frame is pulled, the slope the load-displacement curve increases precipitously with the reduction of θ since $F_2'(x_2) = k_s\left(\sin\theta_0/\sin^3\theta - 1\right)$. When the frame is compressed, the compressive force has a limit when $\sin^3\theta = \sin\theta_0$. In order to have a further increase of the compressive force, we suppose that there are contact pairs at upper and lower corners (lower inset of Fig. 5(a)), leading to a quadric or other form of increase of F_2. Fig. 5(a) shows the force-displacement curve of the scissor-like structural spring. In order to bound the increase rate of spring force, we suppose that the maximum slop $F_2'(x_2)$ is βk_1, where k_1, as already defined, is the spring constant of the contact spring. It should be stressed that the parameter $k_2 = \beta k_1$ is redefined herein to be the maximum increase rate of spring force, $k_2 = \max\{F_2'(x_2)\}$ so that β can be given as a constant in each case study. We thus conducted the simulation based on this non-linear spring and change the additional parameter L to check the size effect of the structural spring. A few results are shown in Fig. 5(b) with $\beta = 1$ and $k_s = k_1/100$. It is shown that the increase of L also leads to small COR and multiple COR minima, which is similar to the cases of linear structural spring with small β. For this non-linear structural spring, the structural response is velocity dependent. General speaking, decreasing L or increasing initial velocity makes the structural spring stiffer in average, resulting in smaller COR. In comparison with the linear case, the α positions of COR minima also shift.

3.3 Effect of many DOFs

Actual structures have multiple DOFs or a spectrum of vibration modes. The effect of multiple vibrational DOFs on COR may partly be investigated using a chain of masses as shown in Fig. 6(a). The case that all masses are identical has been studied by Basile et al. [20]. Here, we work out the scenario that only the mass m_1 is different from others and that all structural springs are identical. Compared with the Two-DOF case, the study of present N-DOF system aims to unveil the influence of internal vibrational DOF

in the mass m_2 in Fig. 1 in the case that m_2 is not a particle but a structure. The detailed formulation and solution is given in the Appendix and the results are shown in Fig. 6(b), in which COR is plotted against $(N\text{-}1)\alpha$. With this plot, the effect of additional (N - 2) DOFs becomes transparent. The general picture on the effect of vibrational DOFs remains the same. It is also found that increasing N leads to more energy storage in the vibrational DOFs, reduces COR and also induces more COR minima. There are a lot of details worth further investigation, which will be addressed in our further work.

3.4 Effect of viscous force

Viscous forces are ubiquitous in dynamical systems, caused by friction and inelastic response of materials. In granular collisions [3], a grain is considered to be viscoelastic since the internal vibration modes can be excited by collision, leading to the transfer of energy from translational motion to thermal vibration. For the above N-DOF system, we have also shown similar results that a portion of mechanical energy is trapped in the vibration modes after impact and that the unity COR does not occur. However, structural vibration is essentially different from thermal vibration, which cannot be regarded as viscous effect directly. In order to study viscous effect, let us attach a dashpot between the two masses, which then establishes the fundamental viscoelastic system. The viscous force is assumed to be proportional to the relative velocity of the two masses, given by $F_v = 2\xi k_2(\dot{u}_2 - \dot{u}_1)/\omega$, where ξ is the damping ratio. For the case of $\beta = 0.001$ (i.e., the contact spring is sufficiently rigid), the numerical results of $\xi = 0.1$, 0.3, 1 and 1.2 are shown in Fig. 7(a). As expected, the results indicate that the more significant damping leads to the smaller COR. For the underdamped cases ($\xi < 1$), the minima of COR more shift to the left when ξ increases. Even for the overdamped cases ($\xi > 1$), a few COR minima can also be discerned, indicating multiple collisions. The left-shift of COR minima indicates that for the same α, an increase of damping ratio ξ may lead to more collisions. This is confirmed by the plot of the number of collision against α as shown in Fig. 7(b). It is further noted that for a given ξ the number of collision peaks at a magnitude of α, beyond which the number of collision reduces and the corresponding COR variation (Fig. 7(a)) becomes smooth. However, the normalized total duration of collision ωt_{col} does not exhibit the corresponding peak, as shown in Fig. 7(c).

Instead, ωt_{col} oscillatory increases with α. In order to unveil why the total duration of collision only increases with α, we look into the details of collision process for cases of large α. Fig. 7(d) shows the dimensionless compression of the contact spring $\omega s_1/V_0$ versus scaled time $\omega t/2\pi$ for the underdamped (ξ = 0.3) and overdamped (ξ = 3) cases respectively. It is noted that the last contact takes the longest time for either ξ, during which the mass in contact m_1 is almost adhered to the wall. Owing to the last contact, the increase of rear mass (namely the larger magnitude of α) undoubtedly leads to the longer duration of the last contact, which has been manifested by the comparison of cases of α = 100 and 200 in Fig. 7(d).

4. Conclusion and Implication

The key message brought up by this investigation is that the COR can be as low as 0.178 if the contact spring is sufficiently stiff and masses in the two-DOF system are particularly distributed. This is not only for the case of two-DOF system but also for at least a chain of masses with N DOFs, as shown in Fig. 6(b). Vibrational DOF does play a significant role in restitution and absorbing kinetic energy, leading to multiple COR minima and the large variation. The main reason for such a dynamical complexity of the simple collision system is that the contact is non-linear by nature. Even the material response is linear elastic, the truncation at the contact response (contact spring can only be compressed) already leads to a large variety of dynamical behaviour. In this sense, we shall emphasis that elastic collision is an ill-posed statement for collisions. Without knowing the details of a dynamical system, we shall not claim COR = 1 simply because of elasticity.

Collision leads to the energy transmission between translational DOFs and vibrational DOFs, which is affected by mass distribution, or the α in the two-DOF system. A small COR system can efficiently transmit energy from translational DOF to vibrational DOF after collision. For the two-DOF model, the most efficient one occurs at α = 0.697, resulting in COR = 0.178. Energetically, it means that that 97% of initial kinetic energy is stored in vibration after collision. This is a striking result, which has not been well recognized by particularly the crashworthiness community. The conventional design of crashworthy structure is established on the notion that a great portion of kinetic energy shall be dissipated through plastic

deformation before restitution. This notion leads to the design of a sacrificing zone at the contact front, e.g., the crush box in a vehicle. The difficulties of such design are the compromise of strength for prolonging the duration of collision and the increase of size for achieving longer stroke of crushing. Our study indicates that the kinetic energy in collision does not have to be dissipated through plastic deformation in a very short time. A large portion of kinetic energy may be stored in vibration, damped out in a long time period and even transformed to the other form of energy (e.g., electricity) during damping. To achieve an efficient energy transmission between translational DOF and vibrational DOF is to design a structure with small COR. This can be achieved by properly distributing masses in the system, exemplified by those particular α values leading to COR minima of the two-DOF system, or increasing vibrational DOFs, exemplified by the *N*-DOF system studied in Section 3.3. Even though the mechanical behaviour of an actual structure can hardly be approximated by a linear spring, very small COR can also be achieved in non-linear system as discussed in section 3.2. Most importantly, utilizing vibrational DOF in absorbing kinetic energy does not contradict with the design of sacrificing zone since the former depends more on how the sacrificing zone is unloaded than how it is crushed, as discussed in section 3.1.

The elastic response of a structure can result in a very small COR if (i) the unloading part of the contact spring is very stiff, and (ii) a particular mass distribution is met. What shall finally be emphasised is that the exact conditions for minimum COR are not difficult to meet but easily overlooked. For two-DOF system, the COR reduces from 1 to 0.178 (82% reduction) when α only reduces from 1 to 0.6971 (30% reduction). With the $\log_{10}\alpha$ scale as shown for example in Fig. 2(a), the distance between two adjacent COR minima reduces when α increases. This indicates that the exploitation of vibrational DOF in absorbing kinetic energy during collision is possible but requires a detailed consideration of vibrational response of the dynamic system.

Appendix

For the N-DOF system as shown in Fig. 6(a), the canonical coordinates are defined as:

$$p_i = \sum_{j=1}^{N} A_{ij} m_j \dot{u}_j \,, \quad q_i = \frac{1}{N} \sum_{j=1}^{N} B_{ij} u_j$$

where

$$A_{ij}=\begin{cases}1, & i=1\\ N-i+1, & j<i, i>1\\ 1-i, & j\geq i>1\end{cases} \text{ and } B_{ij}=\begin{cases}1, & i=1\\ -1, & j=i\\ 1, i>1, & j=i-1\\ 0, \text{othersise}\end{cases}.$$

Note that $p_1=\sum_j m_i\dot{u}_i$ is still the translational momentum of the chain and $\mathbf{A}^{-1}=\mathbf{B}^T/N$ is the condition of canonical transformation, where the superscript "T" indicates transpose. The Hamiltonian is

$$H=\sum_{j=1}^{N}\frac{\left(\sum_{i=1}^{N}B_{ij}p_i/N\right)^2}{2m_j}+\sum_{i=2}^{N}U_i\left(-Nq_i\right)+U_1\left(\sum_{i=1}^{N}A_{i1}q_i-u_0\right)$$

Following the solution for the two-DOF scenario, we assume $\beta=U_i''(x)/U_1''(x)\to 0\,(i\geq 2)$, $U_i'(x)=k_i x$ and write down the kinetic equations for free vibration:

$$-\dot{p}_i=\frac{\partial H}{\partial q_i}=N^2k_iq_i\ \ (i\geq 2) \tag{A1}$$

and kinematic equations:

$$\dot{q}_k=\frac{\partial H}{\partial p_k}=\sum_{j=1}^{N}\sum_{i=1}^{N}\frac{1}{m_jN^2}B_{kj}B_{ij}p_i=\frac{1}{N^2m_2}\sum_{i=1}^{N}\frac{m_2}{m_j}C_{ki}p_i\,, \tag{A2}$$

where

$$\mathbf{C}_{ki}=\sum_{j=1}^{N}\frac{m_2}{m_j}B_{kj}B_{ij}=\begin{bmatrix}N-1+\alpha & \alpha-1 & & & & \\ \alpha-1 & 1+\alpha & -1 & & & \\ & -1 & 2 & -1 & & \\ & & -1 & \ddots & \ddots & \\ & & & \ddots & 2 & -1\\ & & & & -1 & 2\end{bmatrix}, \tag{A3}$$

and we have used the condition that m_i ($i\geq 2$) are identical and $\alpha=m_2/m_1$. Differentiating Eq. (19) with the use of Eq. (A1) renders:

$$-\ddot{p}_i=N^2k_i\dot{q}_i=\frac{\omega^2}{1+\alpha}\sum_{j=1}^{N}C_{ij}p_j\ (i\geq 2), \tag{A4}$$

where $\omega^2=k_2/m_1+k_2/m_2$ defined in the last section is used. Similar to Eq. (5), Eq. (A1) is recast as

$$\dot{p}_i/\omega + Q_i = 0\,,\ (i \geq 2), \tag{A5}$$

where $Q_i = N^2 k_i q_i/\omega$. Noting that p_1 remains unchanged during free vibration and that the symmetric submatrix C_{ij} $(i \geq 2, j \geq 2)$ can be diagonalized with positive eigenvalues and eigenvectors (λ_i, ϕ_{ij}), the solution of Eq. (A4) is obtained under the given condition of the nth collision p_i^{n+} and Q_i^{n+}:

$$p_i = \sum_{k=2}^{N} \left\{ \left(a_k^{n+} \cos(\omega_k \Delta t_n) - \frac{\omega}{\omega_k} b_k^{n+} \sin(\omega_k \Delta t_n) + e_{k1} \frac{\omega^2}{\omega_k^2} c_k^{n+} \left(1 - \cos(\omega_k \Delta t_n)\right) \right) \phi_{ki} \right\} \quad (i \geq 2) \tag{A6}$$

where $\omega_k = \omega\sqrt{\lambda_k/(1+\alpha)}$ is the kth nature frequency of the system, $e_{k1} = (1-\alpha)/(1+\alpha)$ defined in last section is again used. Making use of the normalized eigenvectors $\sum_{i=2}^{n} \phi_{ki}\phi_{li} = \delta_{kl}$, the parameters a_k^{n+}, b_k^{n+}, and c_k^{n+} are respectively given by:

$$a_k^{n+} = \sum_{i=2}^{N} \phi_{ki} p_i^{n+}\,,\ b_k^{n+} = \sum_{i=2}^{N} \phi_{ki} Q_i^{n+}\,, \text{ and } \quad c_k^{n+} = \phi_{k2} p_1^{n+}\,. \tag{A7a, b, c}$$

Using again the inertial frame with velocity $-V_0$, the first collision leads to $p_1^{1+} = 2m_1 V_0$ and $p_{i(i\geq 2)}^{1+} = (N-i+1)p_1^{1+}$. The COR of the system size of N after the first collision is $e_{k1}^{N} = \dfrac{1-(N-1)\alpha}{1+(N-1)\alpha}$, which also reduces with α. Noting that $\dot{u}_1 = (p_1 + p_2)/Nm_1$, the relative velocity between the mass m_1 and the wall at the moment after (n-1)th collision is:

$$\dot{u}_1 - V_0 = \frac{p_1^{(n-1)+} + p_2}{Nm_1} - \frac{p_1^{1+}}{2m_1}\,. \tag{A8}$$

If the nth collision occurs, the momentum change is $\Delta p^{n+} = -\dfrac{2}{N}\left(p_1^{(n-1)+} + p_2^{n-}\right) + p_1^{1+}$, which all goes to m_1. Therefore:

$$p_1^{n+} = p_1^{(n-1)+} + \Delta p^{n+}\,, \tag{A9a}$$

$$p_{i(i>2)}^{n+} = p_{i(i>2)}^{n-} + (N-i+1)\Delta p^{n+}\,. \tag{A9b}$$

The COR after nth collision is then:

$$e_{kn}^{N}=\frac{2p_1^{n+}}{\left(1+(N-1)\alpha\right)p_1^{1+}}-1. \tag{A10}$$

Similar to the case of $N = 2$, we can obtain the minimum value of e_{kn}^{N} by checking the marginal condition of the (n+1)*th* collision, that is at the time of second collision $t_2^{(n+1)-}$:

$$2Nm_1\int_{t_n^{n+}}^{t_n^{(n+1)-}}(\dot{u}_1-V_0)dt=2\left(p_1^{n+}\Delta t_n^{*}+\int_{t_n^{n+}}^{t_n^{(n+1)-}}p_2dt\right)-Np_1^{1+}\Delta t_n^{*}=0, \tag{A10}$$

and the relative velocity between the wall and mass m_1 (Eq. (A8)) vanishes:

$$2\left(p_1^{n+}+p_2^{(n+1)-}\right)-Np_1^{1+}=0. \tag{A11}$$

Since the solution depends on N and eigen-decomposition of the submatrix C_{ij} ($i \geq 2, j \geq 2$), the problem can only be numerically solved with given α and N. The effect of them on COR has been shown in Fig. 6(b).

Acknowledgements

This work was supported by the Department General Research Funds of Hong Kong Polytechnic University. We are grateful for the support.

References

[1] W.J. Stronge, Friction in collisions - resolution of a paradox, Journal of Applied Physics, 69 (1991) 610-612.

[2] W.J. Stronge, Impact mechanics, Cambridge University Press, Cambridge, 2000.

[3] R. Murakami, H. Hayakawa, Effect of elastic vibrations on normal head-on collisions of isothermal spheres, Physical Review E, 89 (2014) 012205.

[4] F. Gerl, A. Zippelius, Coefficient of restitution for elastic disks, Physical Review E, 59 (1999) 2361-2372.

[5] H. Kuninaka, H. Hayakawa, Anomalous behavior of the coefficient of normal restitution in oblique impact, Physical Review Letters, 93 (2004) 154301.

[6] H. Kuninaka, H. Hayakawa, Simulation of cohesive head-on collisions of thermally activated nanoclusters, Physical Review E, 79 (2009) 031309.

[7] P. Muller, M. Heckel, A. Sack, T. Poschel, Complex Velocity Dependence of the Coefficient of Restitution of a Bouncing Ball, Physical Review Letters, 110 (2013) 5.

[8] S. Xu, D. Ruan, G. Lu, T.X. Yu, Collision and rebounding of circular rings on rigid target, International Journal of Impact Engineering, 79 (2015) 14-21.

[9] R.H. Bao, T.X. Yu, Impact and rebound of an elastic-plastic ring on a rigid target, International Journal of

Mechanical Sciences, 91 (2015) 55-63.
[10] G. Kuwabara, K. Kono, Restitution coefficient in a collision between 2 spheres, Japanese Journal of Applied Physics Part 1-Regular Papers Short Notes & Review Papers, 26 (1987) 1230-1233.
[11] K.L. Johnson, Contact mechanics, Cambridge University Press, Cambridge, 1985.
[12] S.C. Hunter, Energy absorbed by elastic waves during impact, Journal of the Mechanics and Physics of Solids, 5 (1957) 162-171.
[13] M.G. Koller, H. Kolsky, Waves produced by the elastic impact of spheres on thick plates, International Journal of Solids and Structures, 23 (1987) 1387-1400.
[14] N.V. Brilliantov, F. Spahn, J.M. Hertzsch, T. Poschel, Model for collisions in granular gases, Physical Review E, 53 (1996) 5382-5392.
[15] T. Schwager, T. Poschel, Coefficient of normal restitution of viscous particles and cooling rate of granular gases, Physical Review E, 57 (1998) 650-654.
[16] R. Ramirez, T. Poschel, N.V. Brilliantov, T. Schwager, Coefficient of restitution of colliding viscoelastic spheres, Physical Review E, 60 (1999) 4465-4472.
[17] N.V. Brilliantov, A.V. Pimenova, D.S. Goldobin, A dissipative force between colliding viscoelastic bodies: Rigorous approach, Epl, 109 (2015) 14005.
[18] N. Brilliantov, T. Pöschel, Kinetic theory of granular gases, Oxford : Oxford University Press, 2004., Oxford, 2004.
[19] W.A.M. Morgado, I. Oppenheim, Energy dissipation for quasielastic granular particle collisions, Physical Review E, 55 (1997) 1940-1945.
[20] A.G. Basile, R.S. Dumont, Coefficient of restitution for one-dimensional harmonic solids, Physical Review E, 61 (2000) 2015-2023.
[21] S. Nagahiro, Y. Hayakawa, Collision of one-dimensional nonlinear chains, Physical Review E, 67 (2003).
[22] M. Hubbard, W.J. Stronge, Bounce of hollow balls on flat surfaces, Sports Engineering, 4 (2001) 49-61.
[23] R. Cross, Impact behavior of hollow balls, American Journal of Physics, 82 (2014) 189-195.
[24] S.J. Haake, C.M. Fau, S.R. Goodwill, The dynamic impact characteristics of tennis balls with tennis rackets, Journal of Sports Sciences, 21 (2003) 839-850.
[25] R. Cross, Dynamic properties of tennis balls, Sports Engineering, 2 (1999) 23-33.
[26] G. Lu, T.X. Yu, Energy Absorption of Structures and Materials, Woodhead, Cambridge, 2003.
[27] N. Jones, T. Wierzbicki, Structural crashworthiness, Butterworths, London and Boston, 1983.
[28] W.J. Stronge, T.X. Yu, Dynamic models for structural plasticity, London ; New York : Springer-Verlag, c1993., London ; New York, 1993.
[29] H.H. Ruan, T.X. Yu, Collision between mass-spring systems, International Journal of Impact Engineering, 31 (2005) 267-288.
[30] J.B. Martin, P.S. Symonds, Mode approximations for impulsively loaded rigid plastic structures, Journal of the Engineering Mechanics Division, proceedings of ASCE, 92 (1966) 43-46.
[31] X.T. Sun, X.J. Jing, J. Xu, L. Cheng, Vibration isolation via a scissor-like structured platform, Journal of Sound and Vibration, 333 (2014) 2404-2420.

1

List of figure captions:

Fig. 1 The two-DOF system for investigating the effect of vibrational DOF on COR.

Fig. 2 COR of the 2-DOF system for a wide range of α: (a) variation of COR against α obtained from both analytical solution for $\beta = 0$ and simulations for finite β; (b) variation of duration of collision with α; (c) variations of the minimum COR and the number of collisions with α; (d) the variation of $(\alpha_n^* - \alpha_n^\#)$ with the number of collision; (e) the comparison of exact and approximate solution for $\beta = 0$.

Fig. 3 The cushion effect of large β: (a) the non-monotonic variation of COR with β; (b) the compression of contact spring versus time.

Fig. 4 The effect dissipative contact spring: (a) the schematic of loading and unloading curves of the contact spring; (b) the effect of nominal dissipation ratio DR; (c) DR = 0.5 and β = 0.01; and (d) DR = 0.5 and β = 0.1

Fig. 5 Effect of non-linearity of structural spring: (a) the scissor-like structural spring and its force displacement relation; (b) the effect of L and the comparison between linear and the non-linear spring.

Fig. 6 (a) A chain of N masses; and (b) the variation of COR with $(N - 1)\alpha$.

Fig. 7 The effect of viscous force: (a) the hard-wall limit ($\beta = 0.001$); (b) Variation of number of collisions with α; (c) Variation of contact time; and (d) the compression of contact spring versus time.

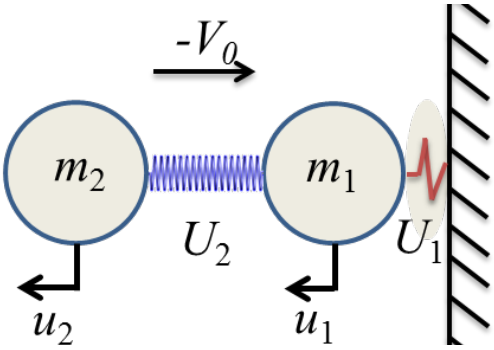

Fig. 1 The two-DOF system for investigating the effect of vibrational DOF on COR

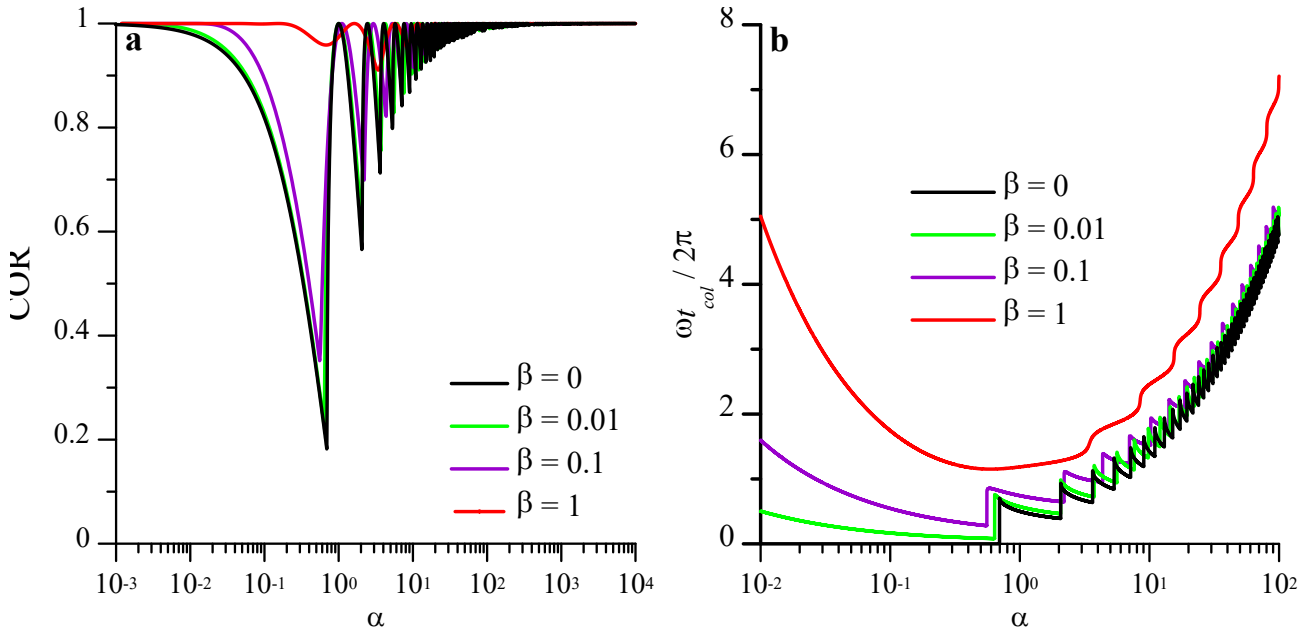
a
COR
α
β = 0
β = 0.01
β = 0.1
β = 1
b
$\omega t_{col} / 2\pi$
α
β = 0
β = 0.01
β = 0.1
β = 1

1

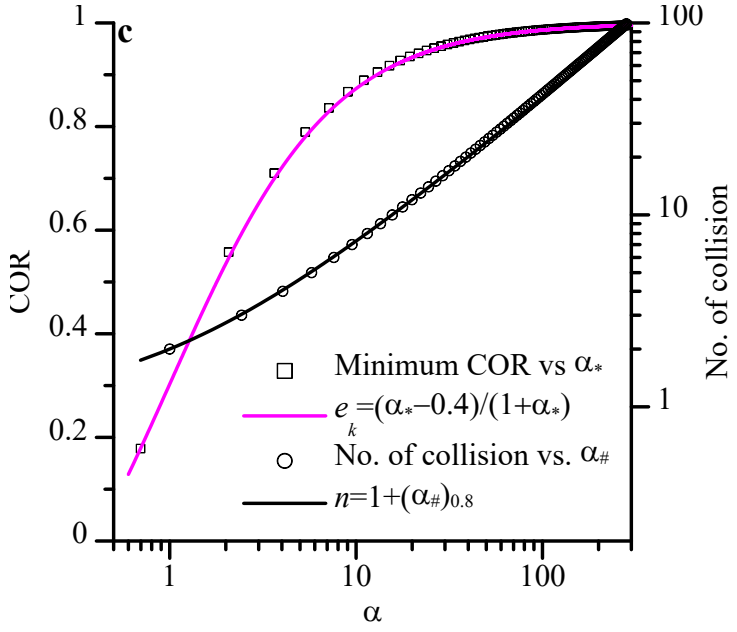
c
COR
No. of collision
α
Minimum COR vs α_*
$e_k=(\alpha_*-0.4)/(1+\alpha_*)$
No. of collision vs. $\alpha_\#$
$n=1+(\alpha_\#)_{0.8}$

2

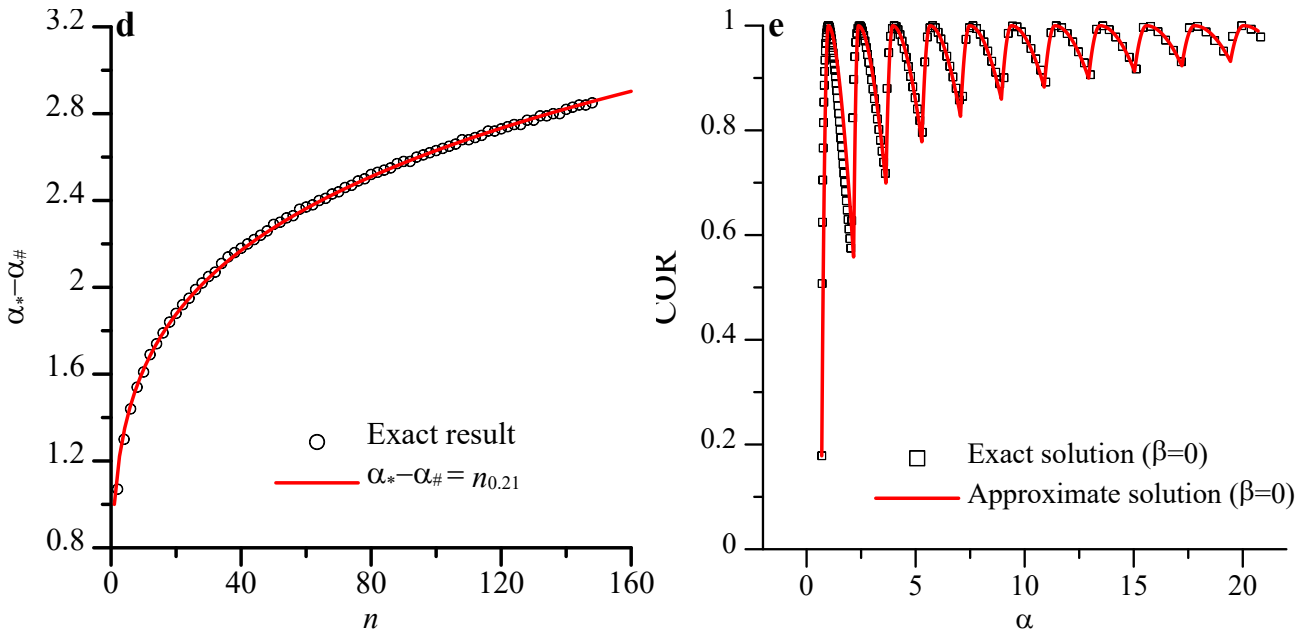

Fig. 2 COR of the 2-DOF system for a wide range of α: (a) variation of COR against α obtained from both analytical solution for $\beta = 0$ and simulations for finite β; (b) variation of duration of collision with α; (c) variations of the minimum COR and the number of collisions with α; (d) the variation of $(\alpha_n^* - \alpha_n^\#)$ with the number of collision; (e) the comparison of exact and approximate solution for $\beta = 0$.

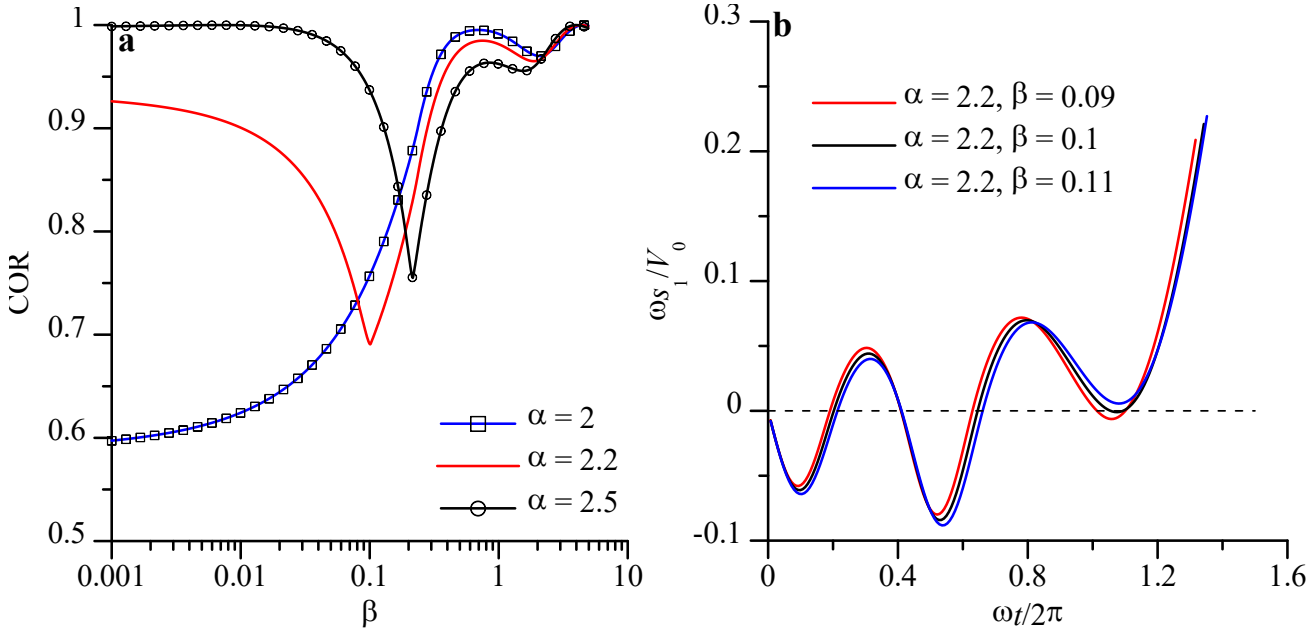

Fig. 3 The cushion effect of large β: (a) the non-monotonic variation of COR with β; (b) the compression of contact spring versus time.

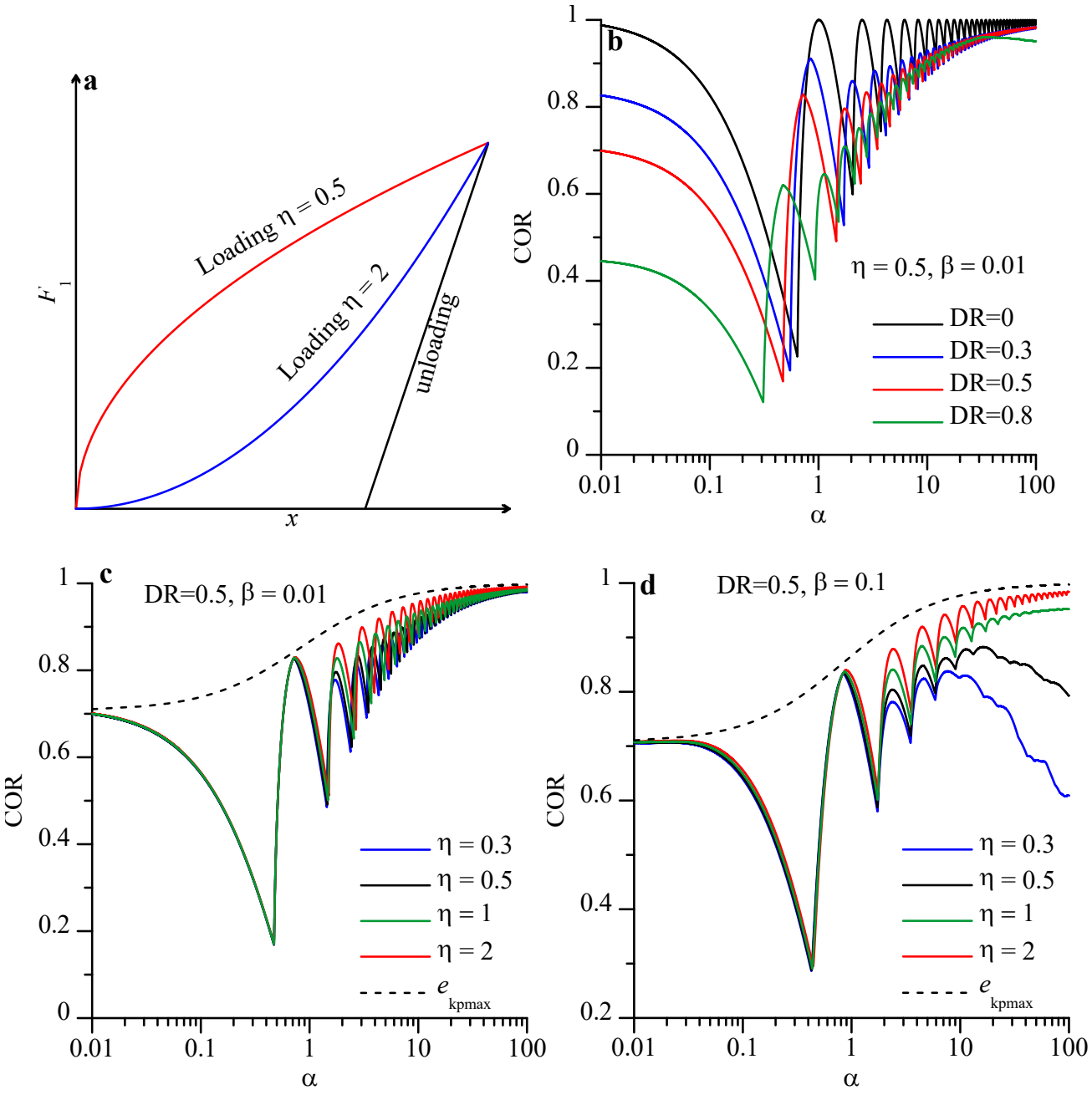

Fig. 4 The effect dissipative contact spring: (a) the schematic of loading and unloading curves of the contact spring; (b) the effect of nominal dissipation ratio DR; (c) DR = 0.5 and $\beta = 0.01$; and (d) DR = 0.5 and $\beta = 0.1$

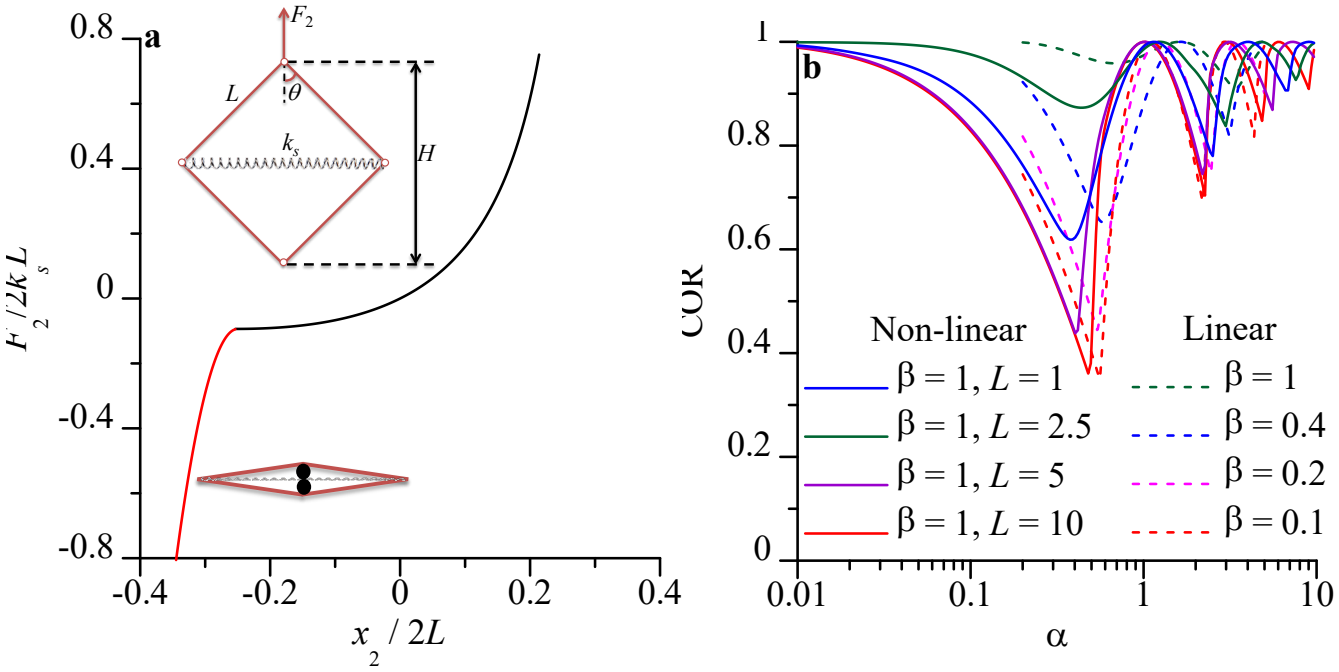

Fig. 5 Effect of non-linearity of structural spring: (a) the scissor-like structural spring and its force displacement relation; (b) the effect of L and the comparison between linear and the non-linear spring.

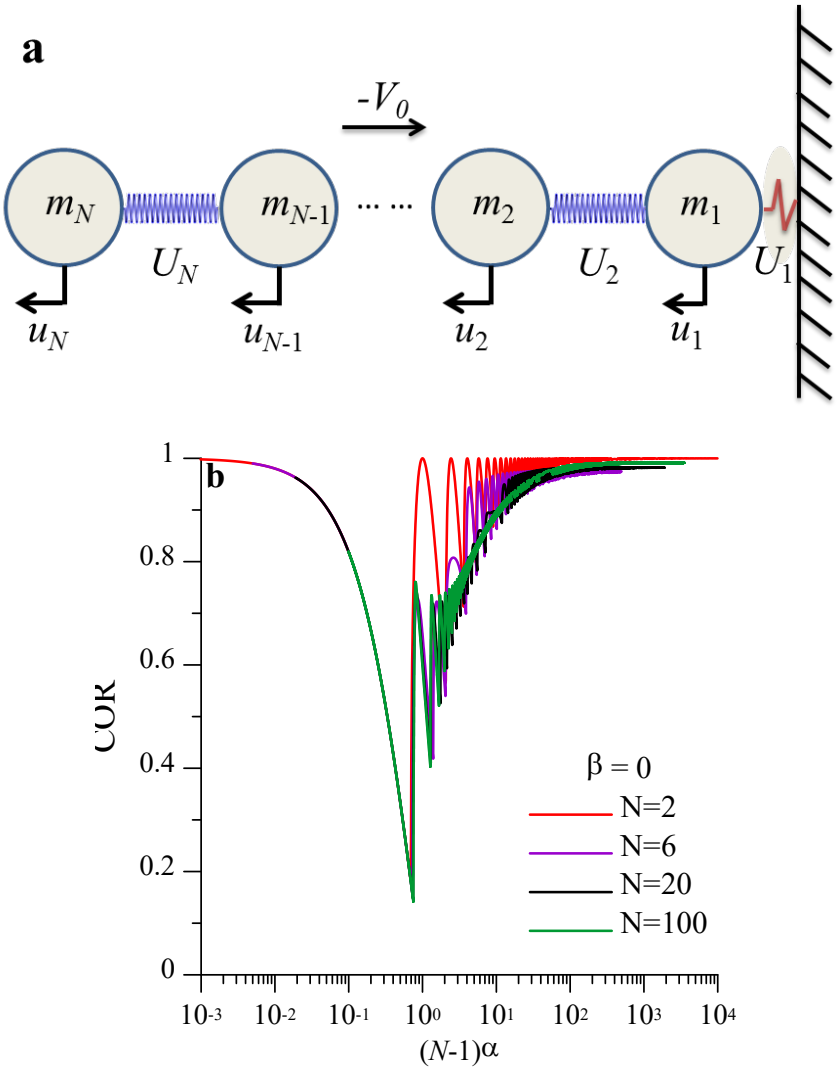

Fig. 6 (a) A chain of N masses; and (b) the variation of COR with $(N - 1)\alpha$.

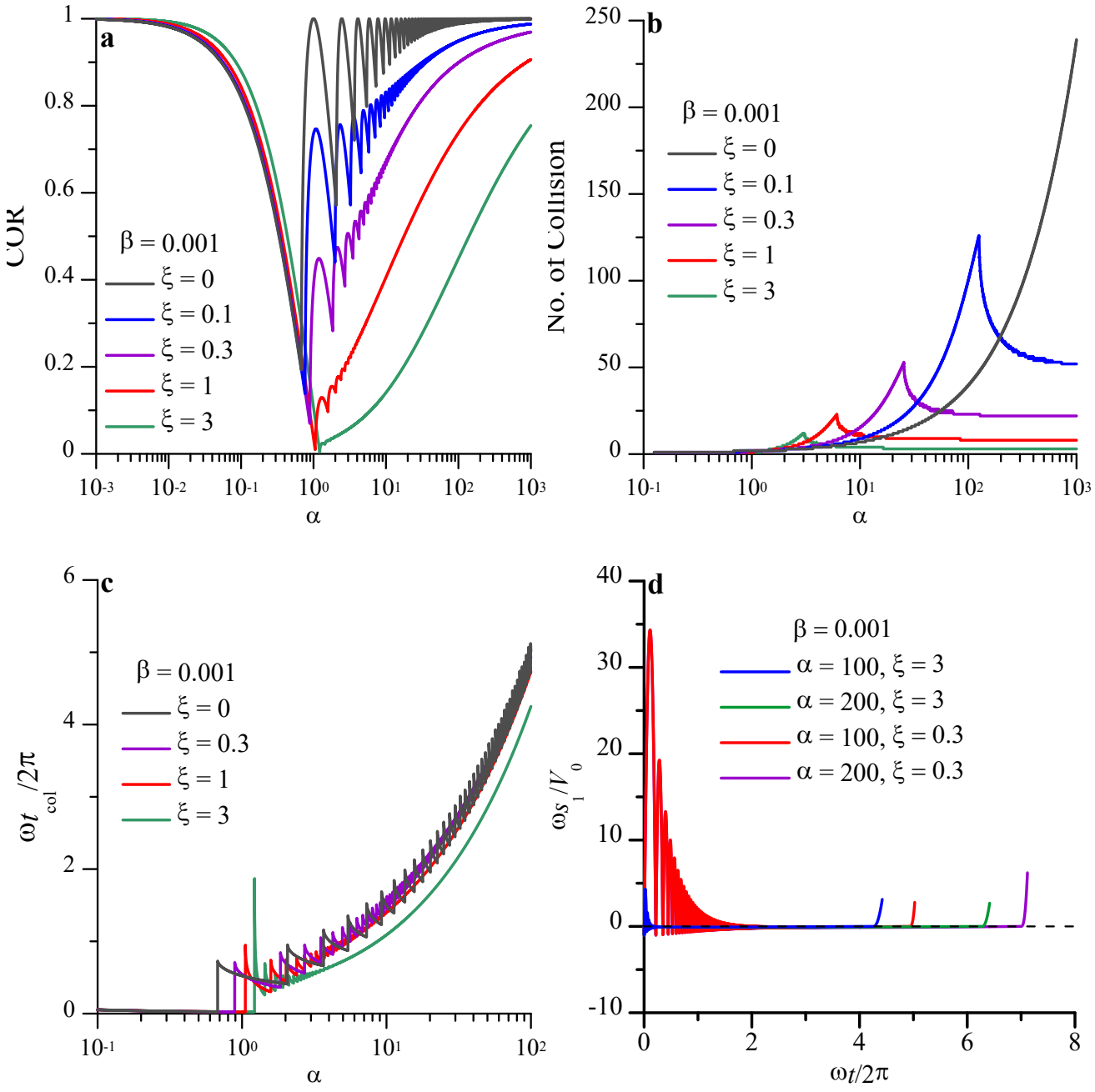

Fig. 7 The effect of viscous force: (a) the hard-wall limit ($\beta = 0.001$); (b) Variation of number of collisions with α; (c) Variation of contact time; and (d) the compression of contact spring versus time.